Journal Profile: ADVANCED ROBOTICS

Journal Information	Value
Full Journal Title :	ADVANCED ROBOTICS
ISO Abbrev.Title :	Adv. Robot.
JCR Abbrev.Title :	ADV ROBOTICS
ISSN :	0169-1864
Issues/year :	24
Language :	ENGLISH
Journal Country/ Territory :	JAPAN
Category :	ROBOTICS - SCIE
Publisher :	TAYLOR & FRANCIS LTD
Publisher Address :	4 PARK SQUARE, MILTON PARK, ABINGDON OX14 4RN, OXON, ENGLAND
Open Access :	NA
Child Title :	NA
Old Title :	NA

Journal Source Data

	Citable Items			Other
	Articles	Reviews	Combined	
Number in JCR Year 2014 (A)	131	0	131	6
Number of References (B)	3,280	0	3,280	2
Ratio (B/A)	25.0	0.0	25.0	0.3

Advanced Robotics

ISSN: 0169-1864 (Print) 1568-5535 (Online) Journal homepage: http://www.tandfonline.com/loi/tadr20

Biologically inspired design of a parallel actuated humanoid robot

Derek F. Lahr, Hak Yi & Dennis W. Hong

To cite this article: Derek F. Lahr, Hak Yi & Dennis W. Hong (2016) Biologically inspired design of a parallel actuated humanoid robot, Advanced Robotics, 30:2, 109-118, DOI: 10.1080/01691864.2015.1094408

To link to this article: http://dx.doi.org/10.1080/01691864.2015.1094408

ADVANCED ROBOTICS, 2016
VOL. 30, NO. 2, 109–118
http://dx.doi.org/10.1080/01691864.2015.1094408

FULL PAPER

Biologically inspired design of a parallel actuated humanoid robot

Derek F. Lahr[a], Hak Yi[b] and Dennis W. Hong[b]

[a]General Motors Global Research and Development, Warren, MI, USA; [b]Mechanical and Aerospace Engineering Department, University of California at Los Angeles, Los Angeles, CA, USA

ABSTRACT

This paper presents the comparison for the role of bi-articular and mono-articular actuators in human and bipedal robot legs, in particular the hip and knee joint, for driving the design of a humanoid robot with inspirations from the biological system. The various constraints driving the design of both systems are also compared. Additional factors particular to robotic system are identified and incorporated in the design process. To do this, a dynamic simulation is used to determine loading conditions and the forces and power produced by each actuator under various arrangements. It is shown that while the design principles of humans and humanoids are similar, other constraints ensure that robots are still merely inspired by humans, and not direct copies. A simple design methodology that captures the complexity and constraints of such a system in this paper is proposed. Finally, a full-size humanoid robot that demonstrates the newfound principle is highlighted.

ARTICLE HISTORY
Received 17 January 2015
Revised 12 July 2015
Accepted 4 September 2015

KEYWORDS
Bipedal robot design; bi-articular actuation; hip and knee joints

1. Introduction

Emergency first responders are the great heroes of our day, having to routinely risk their lives for the safety of others. Developing robotic technologies to aid in such emergencies could greatly reduce the risk these individuals must take, even going so far as to eliminate the need to risk one life for another.[1] In this role, a humanoid robot is a strong candidate, being able to take advantage of both the human engineered environment in which it will likely operate, but also to make use of the human engineered tools and equipment as it deals with a disaster relief effort. In that vein, Shipboard Autonomous Fire Fighting Robot (SAFFiR) is being developed to further the technologies necessary to achieve ultimate goal, in particular we investigate parallel actuation across both the hip and the knee.[2]

There are of course many humanoid robotic designs such as, KAIST University's HUBO,[3,4] Honda's ASIMO,[5] Waseda University's Wabian-2,[6,7] and Technical University of Munich's Johnnie and LOLA,[8–10] and all have significant achievements to their name. They also share many similarities in how they are actuated. Specifically, nearly all of the aforementioned designs rely on harmonic drives for speed reduction between the motor and the joint, which tend to force researchers to design humanoid limbs as serial manipulators.

This approach is in stark contrast with the biology of a human leg. For example, the human body employs a highly over-actuated and parallel architecture. Specifically, the mechanical coupling of actuators extends up and down the whole leg.[11] It is our goal to understand the effectiveness of such an arrangement and apply it to humanoid robot design.

In that vein, SAFFiR was designed to break out of this mold and investigate and take advantage of a parallel architecture employing linear actuators.[12,13] It is hoped that this new parallel architecture will enable more robust performance in difficult environments in which SAFFiR and other future emergency response robots are expected to operate. This paper will compare human and robot actuation methods, the design of the SAFFiR (with emphasis on the lower body), as well as experimental results from walking tests which validate the parallel actuator arrangement.

2. Background of humanoid design

By their very nature, human beings and humanoid robots undertake very similar actions, including standing, walking, and jumping. However, the means by which their actuators and skeleton accomplish these actions are very different. This is in part due to the nature of the 'technology' within. Because the type, characteristics, and control of each actuator are different, the way in which they are implemented is also different.

The muscular–skeletal arrangement of a human leg has effectively the same number of degrees of freedom as a humanoid. However, the biological leg uses extensive

CONTACT Hak Yi yihak@ucla.edu

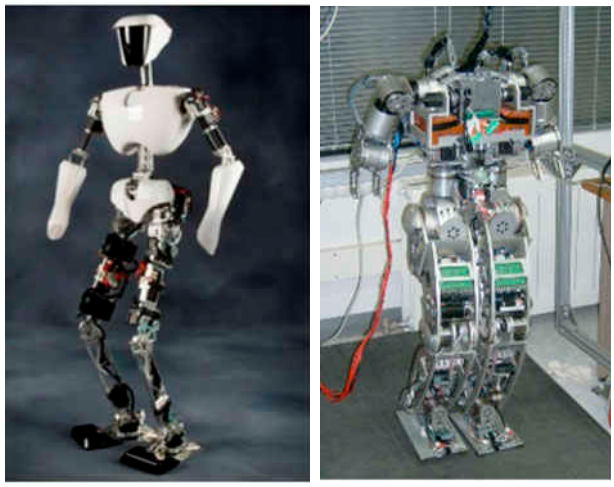

Figure 1. Cognitive humanoid autonomous robot with learning intelligence, CHARLI on left, and HUBO from KAIST on right.

parallel actuation, while humanoids are almost strictly serially actuated. Among a variety of explanations for this difference, we will focus on inspiration and design principles from the human leg in order to build a better robot leg. In this section, the primary characteristics of both humanoid and human leg are discussed and areas of improvement for humanoids highlighted.

Existing humanoid robots stand out as widespread exposure and higher sophistication presents a good indication of the available technology. To emphasize the importance of the hip and knee design, this section will focus primarily on those portions of humanoid robots in existence. It will be seen that due to the demanding and often antithetical constraints of these robots (a lightweight, high-strength, and powerful robot), similar designs have been reached by their builder. In general, all humanoid legs include either 6 or 7 DOFs with DC motors, harmonic drive units, and belt reductions, as seen in Figure 1.

2.1. Hip joint

Like the human hip joint, all bipedal robots are primarily designed with three DOFs at the hip. Such a hip joint uses three revolute joints whose axes intersect at a point to allow a more compact configuration and more human like proportions. Considerable effort into the mechanical design of the hip joint has led to increased performance. For example, both HUBO and Wabian-2 employ harmonic drives mounted on the hip joint which are driven through a toothed belt by DC motors. The hip yaw axis of LOLA is inclined toward the vertical axis of the robot for better power distribution.[9]

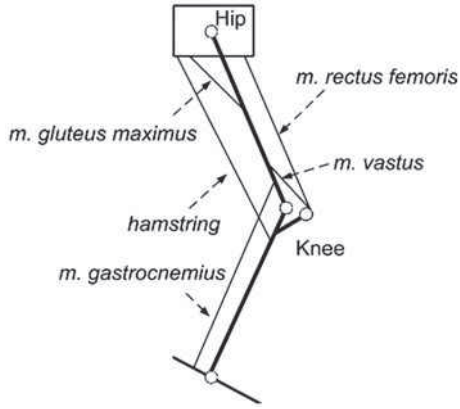

Figure 2. The major muscle groups of the hip and knee.

2.2. Knee joint

The human knee joint is one of the simpler joints within the body, but it also requires the most power among all leg joints. Furthermore, the knee joint on a humanoid must retain the capability of both high speeds and large torques. To reach this level of performance, ASIMO utilizes an electric motor driving a harmonic drive unit through a toothed belt.[4] Compared to both HUBO and Wabian-2, the longer belt allows the motor to be mounted as high on the thigh as possible, thereby reducing the moment of inertia of the leg. The HUBO knee joint driven by two smaller 150 W motors satisfy the high power-to-weight ratio.

The one noteworthy exception to this trend is LOLA, which is equipped by a ball screw actuator on the knee.[9] A linear actuator on LOLA is employed for better mass distribution, compared to one of HUBO and Wabian-2. As joint mass increases, the moment of inertia in the knee also increases. This in turn requires a large part of the hip joint torque to accelerate a heavier thigh.

3. Parallel actuation in human body

The anatomy of human body is not built in the same way. Instead of serial actuation, the hip, knee, and ankle joints are driven in parallel by dozens of major muscles.[14] Of those, more than 20 directly exert torques on the hip joint. The major muscle groups that control the pitch axes of the hip and knee can be seen in Figure 2. Those include the *m.gluteus maximus*, hamstring, *rectus femoris*, and *m. vastus*. Notable is the fact that two of these muscles, the hamstring and the *rectus femoris* are bi-articular. Both muscles span more than one joint, the hip and the knee.

It has been shown that these bi-articular muscles are responsible for transferring power between the joints especially during powerful motions such as jumping.[15] In

general, human can move across various irregularities by running, considered as continuous jumping. So this study applies the jumping model for considering the maximum load and fast speed of robot walking. In [15,16], it has shown that approximately 300 W of power flows through the *m. rectus femoris* to the knee joint in the preflight extension of a leg while jumping. In doing so, this muscle has constant length, and therefore produces no power of its own. The trend continues to the ankle via the *m. gastrocnemius*, which delivers 200 W from the knee to the ankle.

The humanoid SAFFiR uses a bio-inspired design of muscle-like linear actuators arranged in parallel around a multi-DOF joint. The goal of this work is to represent the complex parallel actuated joints, including bi-articular actuation, and use that representation to understand the effects of a bio-inspired architecture on humanoid legs.

3.1. Contribution

The ability to transfer power is a valuable one. This is particularly true in humanoid robots, where a load of either one or two joints is much heavier than others, (hip roll and knee pitch).[3,5] Incorporating biologically inspired bi-articular actuators to humanoid legs can allow them to better distribute loads and power across several actuators and therefore overcome the traditional limitations on joint actuation typical of serial actuated robots.[2,17,18] There are a handful of robot designs that make use of bi-articular actuators.[16–18]

Our contribution to this area is a better understanding of the mechanics and constraints important to parallel and bi-articular actuators in humanoid robots, especially as they compare to humans. We also adopt a simple method of representing such complex systems.[19] This representation lends itself toward optimization in that physical design constraints are easily defined. A physical implementation of a more simple and robust parallel design is shown as part of a full-size humanoid robot.

4. Method

In this work, we focus on two of the three leg joints, the hip and knee. They are chosen and the ankle is except for two reasons. The first is that the knee joint is the most heavily loaded leg joint. Because humanoids most often walk in a bent knee configuration, the weight of the robot regularly exerts large torques across the knee in single support. Similarly, the hip roll joint in general supports large torques due to the center of gravity's (COG) position with respect to the hip joint. This joint though does not usually produce much power. It is therefore a good candidate to deliver power to the knee through bia-

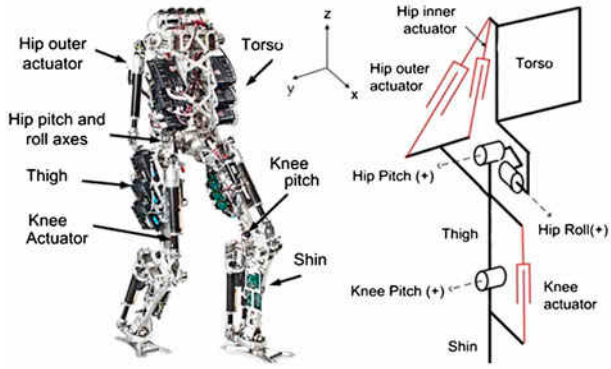

Figure 3. The developed lower body of SAFFiR (left) and kinematic arrangement of its right leg (right).

rticular actuation. Finally, the ankle is not considered for simplicity and because for typical robot actions, it generates little torque or power and instead is primarily used as a stabilizing joint.

The design of any system begins with the characterization of all the loads that it will see. In this paper, we look primarily at the action of jumping, specifically the loading phase of a jump prior to lift-off. Jumping places both large loads and demands high power from both the hip and the knee. A design that can sustain jumping will likely suffice for most other actions a humanoid will make. Motions such as walking and climbing stairs actuate similar actuator groups but typically require lower power outputs. The jumping motion is used because it is both easy to model and is representative of the maximum motor power requirements.

As mentioned above, for simplicity we will be studying the interplay between three DOF in various actuator configurations. The three DOF are the hip roll, hip pitch, and knee pitch, as seen in Figure 3. There are three actuators, one for each DOF, and any or all can be arranged in a bi-articular fashion across the hip and knee. This study is limited to only three particular cases, which are the most helpful and most easily implemented.

A cable pulley arrangement allows these arrangements to be feasible, as seen in Figure 6. Instead of mounting directly to the robot link, such as the thigh or shank, the actuators are instead mount to a lever, rigidly attached to a pulley. Fixed to the pulley are two cables, each extending down the link to another pulley fixed to the following link. This arrangement allows for shorter actuators, both positive and negative leverage ratios, and more design parameters (pulley radii etc.)

We adapt a kinematic model of parallel manipulators to describe the otherwise complex interactions.[9,19] The model relates the linear force produced by the actuators to the torque generated about each joint, as seen in

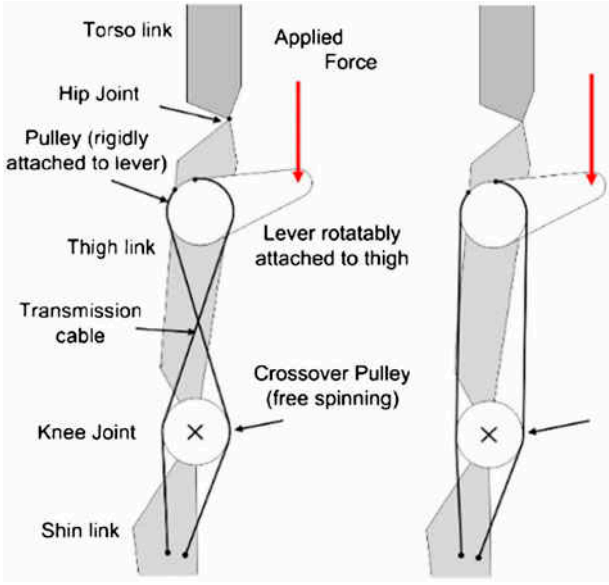

Figure 4. Two implementations of the thigh actuator as a bi-articular one. The configuration on left shows a negative leverage ratio, while the one on right more closely resembles its biological counterpart.

Equation (1):

$$\tau = \begin{bmatrix} \tau_x \\ \tau_y \\ \tau_z \end{bmatrix} = G \cdot f = \begin{bmatrix} g_{1,1} & g_{1,2} & g_{1,3} \\ g_{2,1} & g_{2,2} & g_{2,3} \\ g_{3,1} & g_{3,2} & g_{3,3} \end{bmatrix} \cdot \begin{bmatrix} f_x \\ f_y \\ f_z \end{bmatrix} \quad (1)$$

where f is a vector of linear actuator forces and τ is a vector of joint torques. With three actuators and three joint torques, the matrix G will be 3×3 where each column can be thought of as the torque generated about each joint due to one Newton of actuator force. For the remainder of the work, the first column represents the hip outer actuator, second column the hip inner actuator, and third column the knee actuator. Therefore, each element of G can be computed as in Equation (2):

$$\tau = z_m \cdot \left[r_{m,n} \times u_n \right] \quad (2)$$

where z_m is the unit vector in the direction of the mth joint, $r_{m,n}$ is the vector from the center of the mth joint to the center-line of the nth actuator, and u_n is the unit vector in the direction of the nth actuator.

In doing so, the model nicely captures the geometry of the whole system. Furthermore, the principle of virtual work allows us to derive Equation (3):

$$v = G^T \cdot \omega \quad (3)$$

which relates the angular velocity, ω, of the joints to the linear velocities of the actuators, v.

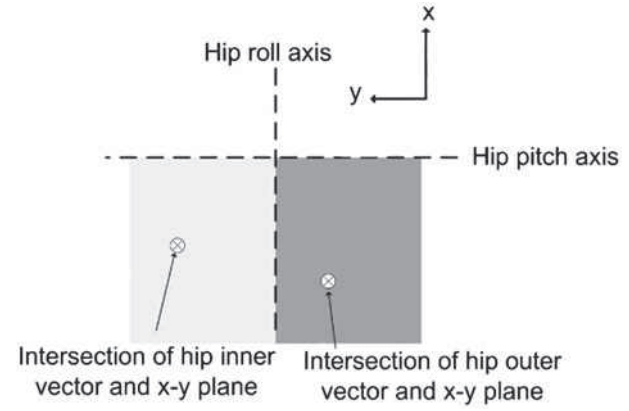

Figure 5. Actuators 1 and 2 are assumed to be on the same side of the pitch axis and opposite sides of roll axis. Illustration shows the top view.

Similarly, the inverse of either Equations (1) or (3) provides the opposite relationship, from torques to forces and linear to angular velocities. For this analysis, we make the assumption that the torque generated by each actuator does not vary with the joint position. For most motions, the robots joints range is limited such that this approximation is still representative. Finally, this approach can be easily extended to the full leg of the robot.

We are interested in understanding the function and optimal use of the three candidate bi-articular configurations in the design as they apply to humanoid robots. Referring to Figure 5, we will now define G and establish constraints on its values. Actuator one and two always extend across the hip roll and pitch joints. Their position is limited by packaging constraints as well as the need to actuate both roll and pitch axes. Therefore, we constrain outer hip actuator to the $-y$ side of the hip, reflected by the minus sign on element (1, 1). The inner hip actuator also crosses the hip but is opposite actuator one with respect to the roll axis. Both are nominally behind the hip, so the sign on elements $g_{2,1}$ and $g_{2,2}$ are positive. It can be shown there is no loss of generality in these constraints. Actuator three nominally crosses the knee at a positive x position.

There are up to nine variables to adjust. To isolate the effect of bi-articular configurations we fix the value of elements $g_{1,1}$, $g_{1,2}$, $g_{2,1}$, $g_{2,2}$, and $g_{3,3}$ to their nominal value. In this case, we set the torque generated by the actuators across their respective axes to approximately 0.05 Nm/N.

By making elements, $g_{2,3}$, $g_{3,1}$, and $g_{3,2}$ non-zero, we can represent bi-articular actuators (one that spans both the hip and knee). Furthermore, we constrain the value of these elements to scalar functions of the same actuators leverage on the opposite pitch joint, as indicated by the p_n terms of Equation (4). In practice, these linear scaling

Table 1. Peak torque and angular velocities during jumping motion.

Joint	Hip roll	Hip pitch	Knee pitch
Peak torque	−33 Nm	−20 Nm	70 Nm
Angular velocity	0	1.65 rad/s	−1.65 rad/s

factors, p_n, are analogous to the pulley radii, as seen in Figure 4. In this study we will be varying the sign and magnitude of these elements to understand their effect on the actuator force and power requirements during jumping.

$$\tau = G \cdot f = \begin{bmatrix} -0.05 & 0.05 & 0 \\ 0.05 & 0.05 & 0.05p_3 \\ 0.05p_1 & 0.05p_2 & -0.05 \end{bmatrix} \cdot f \qquad (4)$$

4.1. Jumping model

A jumping motion is used as a representative loading on a humanoid leg. This motion is chosen because it includes a high load phase during the initial acceleration as well as a phase of high joint velocities, immediately prior to take-off. Finally, it has the benefit of being easy to model in the early stages of the robots development. Jumping loads are generated by simulation using a SimMechanics® model. We use a link model to represent the torso, thigh, and shank. The foot is considered fixed to the ground, however foot reaction forces are computed such that they obey the unilateral constraints of ground contact as well as the friction cone constraints.

The model begins from a crouched position with the COG over the ankle. The joint trajectories are defined to maintain the COG in this position within a tolerance of 10 mm. The torques generated about the hip roll, pitch, and knee pitch are computed via the built in ODE solver. The approximate peak values are given in Table 1.

5. Results

In this section, we will look at two configurations, one in which the outer hip actuator is bi-articular, and one in which the inner hip actuator is bi-articular. In both cases, the knee is also bi-articular. Therefore, we investigate the effect of the pulley ratios on the distribution of forces and power across the actuators. We draw trends from both these results based on both force and power constraints.

Two metrics are used to assess the results. First is the sum of squares of actuator forces generated during the jumping motion. Second is the sum of the absolute value of the mechanical power produced by each actuator. These are represented in Equations (5) and (6), respectively. Therefore, the ideal configuration would be one

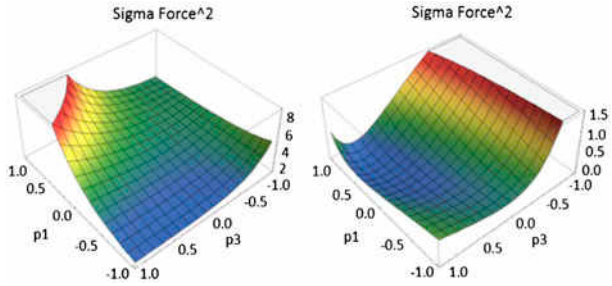

Figure 6. Sum of squares of power and force across all three actuators at various pulley ratios, p_1 and p_3. Hip outer actuator is bi-articular.

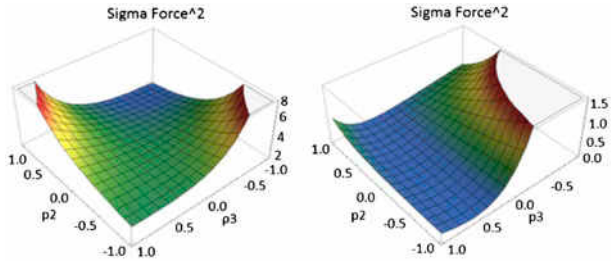

Figure 7. Sum of squares of power and force across all three actuators at various pulley ratios, p_2 and p_3. Hip inner actuator is bi-articular.

with low forces and low power, indicating that actuator loads are small and only positive power is generated. These metrics are presented when the hip outer actuator is bi-articular in Figure 6. These results are generated under the conditions in Table 1. The variation is plotted against the pulley ratios p_1 and p_3, thus the hip outer actuator is bi-articular. The best distribution of power occurs when p_1 and p_3 approach 1. In this configuration, all actuators produce positive power close to 30% of the total power. Absolute forces are lowest though when p_1 is close to 1 and p_1 nears −1. There is a trade-off then between optimally low forces and optimal power distribution. Interestingly, much like a human's *m.rectusfemoris*, the knee power is zero when $p_3 = 1$. At this ratio, the knee actuator acts as a rigid link, transmitting forces up to the hip pitch joint.

$$\sigma_f = (G^{-1} \cdot \tau)^2 \qquad (5)$$

$$\sigma_p = (G^{-1} \cdot \tau * G^t \cdot \omega)^2 \qquad (6)$$

Figure 7 shows the same variation but when the inner hip actuator is used as the bi-articular actuator and the outer hip is only mono-articular. Again, when $p_3 = 1$ the knee actuator performs no work. Furthermore, it can be shown that the inner hip actuator only performs negative work in this case. The best distribution of power occurs

when $p_3 > 0$ across a range of p_2 values, however unlike above, one actuator is performing negative work. Absolute forces are minimized across actuators when $p_3 = -1$ and $p_2 = 1$. Interestingly, in this configuration, optimal power and optimal force distribution points are closer, and a compromise may be easier to find. If efficiency is of utmost importance, this configuration is less desirable than above because of the negative work performed by the inner hip.

A human hip and knee operates with two bi-articular and two mono-articular muscles. The hamstring and *m. rectus femoris* cross both the hip and the knee. Both are arranged such that the torque generated on both joints is in the same direction. This is analogous to a pulley ratios of $p_3 = 1$ and $p_2 = 1$. Both muscles serve to redistribute power. The hamstring moves power from the knee to the hip, and the *m. rectus femoris* transmits power from the knee to the hip. Overall though, there is a net gain in power at the knee.[20] The above analysis would indicate that the human is more likely to be configured for best energy distribution at the cost of high muscle forces. Furthermore, these muscles have likely evolved to transmit large loads but generate little power. Similarly, when robotic actuators are custom designed for their specific application, the entire system can benefit.

The above results show significant variation in results when just adjusting two parameters. A full optimization is required to attain best results. Fortunately, the representative model suggested above provides a convenient framework for such an optimization without dealing directly with actuator end point locations or kinematics.

The results of such an optimization will be the subject of future work. Although an optimization is not within the scope of this work, some considerations are given. First, it is important to fix and/or constrain the elements of G. For example, elements $p_{1,1}$ and $p_{2,1}$ can be related linearly, as can $p_{2,1}$ and $p_{2,2}$. Element $p_{2,3}$ should also be fixed at a nominal value. If these constraints are not enforced, the simulation will simply reduce their values to minimize actuator forces.

6. SAFFiR design

6.1. Overview

This work investigates the effect of various configurations of parallel actuation across the hip and knee of a humanoid robot. The above results have one particularly interesting point in common, when all pulley ratios are zero. As seen in Figures 6 and 7, this point shows both moderate forces and power. Furthermore, this configuration has the benefit of being the simplest to mechanically implement (an important consideration when designing an already complex system such as a humanoid from the ground up). Using qualitative results from the study above, the authors designed, built and tested this configuration in the form of our new humanoid SAFFiR, as seen in Figure 8. Furthermore, the parameterization represented by Equation (1) is used to ensure actuator forces are not exceeded during common expected motions.

The SAFFiR is a 33 DOFs humanoid robot that includes two 6 DOF legs and arms, a 1 DOF waist, 2 DOF neck, and 3 DOF hands, as shown in Figure 8. The general proportions of the robot and the range of motion, power, and approximate reduction ratio of each DOF can be seen in can be seen in Tables 2 and 3, respectively.

6 DOFs are used in the legs to make the feet fully independent of the torso, allowing for complete control of the torso while in single support. The same is true of the arms, which provide 6DOFs to the hands. Three DOF hands are notionally used, having three one DOF fingers. The robot is primarily fabricated from 6061 Aluminum because of the materials high strength-to-weight ratio and ease of machining as compared to other Aluminum alloys. Each skeletal joint of the lower body is supported by two preloaded angular contact bearings to ensure there is no play in the structure. The joints of the upper body ride on preloaded cross roller bearings in each DOF.

The SAFFiR architecture employs both a unique actuator and actuator arrangement to achieve new gains in mobility and agility as compared to conventional humanoid robots. The parallel actuation architecture (in which one joint comprised of several DOFs is spanned by an equal number of actuators) is used to enable higher torques and power in certain motions, improve positional accuracy, and reduce backlash.

6.2. Hip joint

As alluded to earlier, the hip joint employs a hybrid parallel/series arrangement. The yaw DOF is driven directly by one actuator, while the pitch and roll DOFs are parallelly driven by two linear actuators. The hip pitch and roll typically require more power, torque, and precision than the yaw, and so were chosen to be driven together to maximize the benefit of parallel actuation during a walking cycle. The highest power draw occurs about pitch during the accelerations of the leg swing, while maximum torque is needed for the stance roll joint to support the remainder of the robot. Because of the length of the leg, the precision of the roll and pitch have a greater effect on foot placement than yaw, as seen in Figure 9.

The two linear actuators of the hip drive the pitch and roll DOFs through two effective levers (defined as the perpendicular length between the actuator and the axis of rotation). The roll levers are maximized to provide a

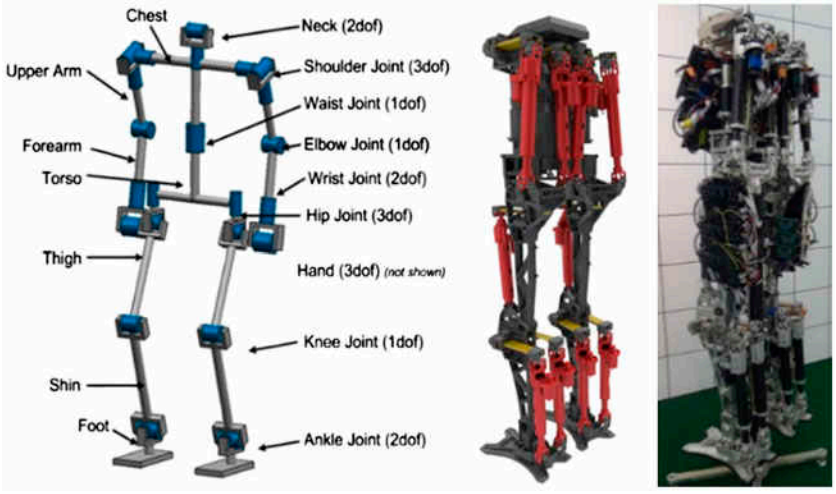

Figure 8. Full kinematic arrangement (left), Actual (middle), and CAD (right) model of SAFFiR's lower-body.

Table 2. Length specifications of SAFFiR.

	Tall height	Thigh	Shin	Foot height	Hip width	Shoulder width	Upper arm	Lower arm
Length (mm)	1600	380	380	40	195	460	250	200

Table 3. Range of motion, mechanical advantage (between motor and limb), and power of SAFFiR's leg joints.

	ROM (deg)	Peak power (W)	Peak gear reduction
Hip yaw	−25, 10	100	230:1 Planetary
Hip roll	−23, 23	400	320:1 Ballscrew
Hip pitch	−45, 45	400	350:1 Ballscrew
Knee pitch	0, 90	200	370:1 Ballscrew
Ankle pitch	−40, 50	200	350:1 Ballscrew
Ankle roll	−20, 20	200	180:1 Ballscrew

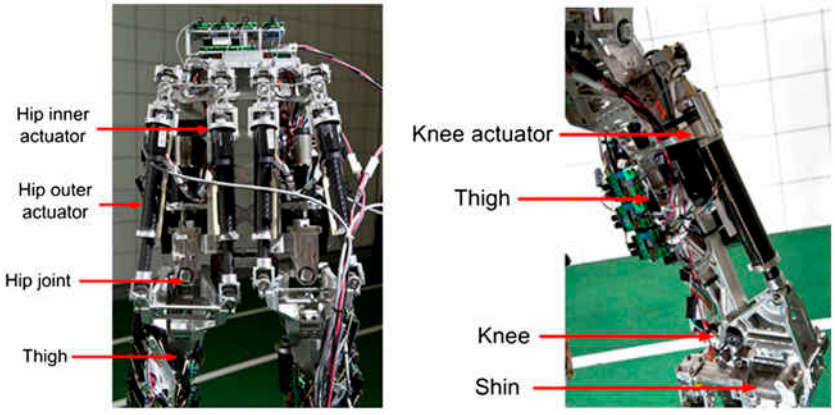

Figure 9. Parallel hip actuators (left) and knee actuator (right) on the SAFFiR.

large degree of torque about this axis while keeping interferences from occurring. With a hip width of 190 mm, the roll lever was made 65 mm long for a gear reduction of 320:1. The lever arm for pitch was made slightly longer as there were fewer packaging constraints. It is 70 mm long for an overall reduction of 350:1.

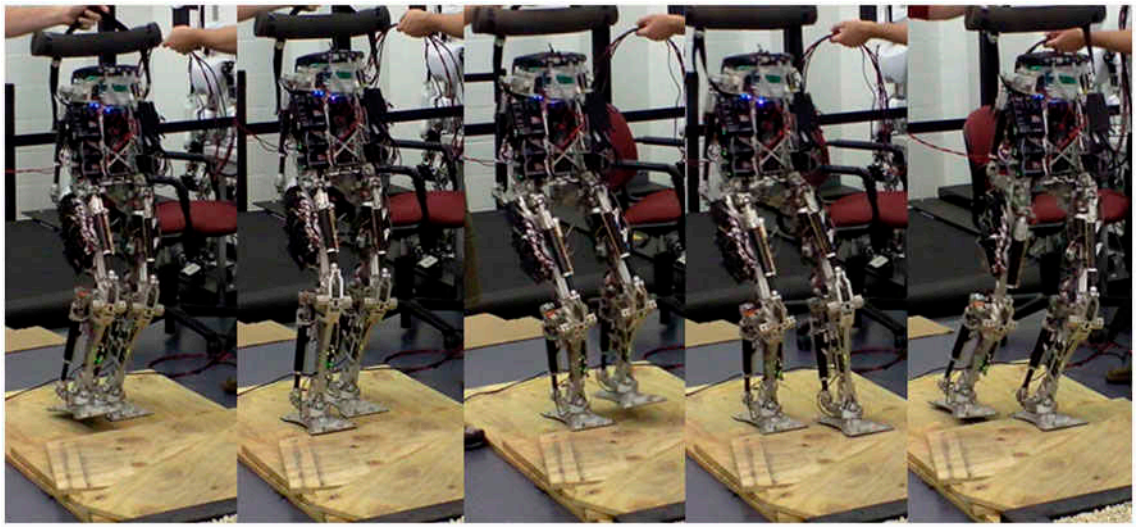

Figure 10. SAFFiR striding across strewn plywood.

6.3. Knee joint

The knee is more straightforward than the hip. The knee is driven by a 200 W linear actuator to handle the higher power and force output required by certain motions such as bent knee walking or squatting. As is, this motor operates at roughly 40% of its continuous capability, indicating the motor is properly sized considering more weight will be added to the robot as it develops. The lever arm for the knee is 75 mm long and is biased so that when the knee is bent, the mechanical advantage increases, and when straight, the advantage decreases. This allows for greater knee speed when walking, and more torque when bent for squatting.

6.4. Preliminary walking tests

A preliminary walking algorithm has been implemented on the robot, the algorithm uses simple time based trajectories generated online in conjunction with knee and hip feedback strategy based on the gyro rates to improve stability. While the algorithm is not particularly noteworthy (and so not detailed here), some of the results are. The forces generated in each actuator from one leg were measured during two strides and are presented in Figures 10 and 11. In this figure, dual support and single support phases are denoted by DS, and SS, respectively. The blue line represents the inner actuator, and the red line the outer actuator. Positive values signify the actuator is in tension.

Most notable from this plot is the distribution of force between the two hip actuators during the first single support phase in which the right leg is the stance leg. Firstly, it is during this phase that the maximum loading of the hip

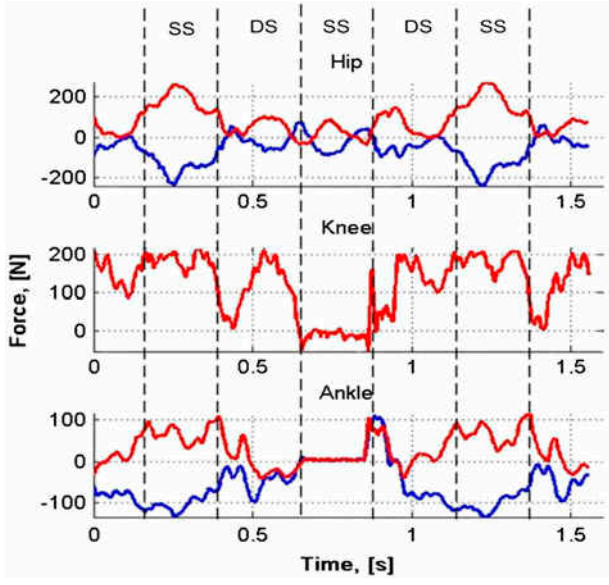

Figure 11. Actuator forces as a function of time for the right hip, knee, and ankle during a walking stride.

actuators occurs. Secondly, the actuators are nominally acting in equal and opposite directions, meaning the hip is predominantly loaded about the roll axis. The magnitude of the roll torque matched the expected value given the robots weight, hip width, and acceleration.

Around 0.2 s, the left leg lifts from the ground and the robot goes into single-support phase with the right leg acting as the stance leg. The left heel strikes the ground at 0.4 s and momentarily unloads the right knee; the double-support phase follows. Both the knee and ankle plots go to zero during the next single-support phase when the right leg is in the air. The right heel strike is clearly visible at 0.9 s in both the ankle and knee. The effort of each

actuator to meet the loading requirements of the hip is minimized, which prolongs battery life and increases the load carrying capability of the robot.

7. Conclusion and future work

In this paper, we investigated an application of biologically inspired parallel actuation of a humanoid robot with emphasis on the lower body. Various configurations of parallelism were studied that included both bi-articular and mono-articular actuators. A representation was adopted from parallel manipulators to concisely capture the otherwise complex design. Furthermore, this representation lends itself very nicely to prescribing constraints on such a system when optimizing. The analysis of two configurations showed that while the design principles of humans and humanoids are similar, other constraints ensure that robots are still merely inspired by humans, and not direct copies. In particular, the analysis shows that more specialization of actuators is needed to allow for more energy efficient designs, especially with regards to the actuator load capacity. A full-size humanoid robot that demonstrates the benefit of parallel actuation and the promise of biologically inspired designs is highlighted. Walking tests showed the expected optimal distribution of forces across hip actuators.

Disclosure statement

No potential conflict of interest was reported by the authors.

Funding

This work is supported by ONR through [grant number N00014-11-1-0074]; [grant number N00014-15-1-2064], and DARPA through [grant number N65236-12-1-1002].

Notes on contributors

Derek F. Lahr received his BS degrees in Mathematics and Mechanical Engineering at Virginia Tech. He continued his graduate studies there in the field of robotics and mechanisms. He received his MS and PhD degrees in 2009 and 2014 at Virginia Tech. His research interests lie in the areas of kinematics, dynamics, and controls, and have been supported by the NSF, ONR and DARPA. He holds two US Patents for his inventions in continuously variable transmissions and currently works for General Motors Research and Development.

Hak Yi received his BS and MS degrees in Mechanical and Aerospace Engineering Department from Chonbuk National University (2005, 2008), and his PhD degree in Mechanical Engineering from Texas A&M University-College Station (2012). Since 2013, he has been a postdoc researcher at the Robotics & Mechanism Laboratory at Virginia Tech and UCLA. His research interests lie in design and bio-inspired control of a variety of bipedal robots.

Dennis W. Hong a TED alumnus, is a professor and the director of Robotics & Mechanisms Laboratory within the Mechanical and Aerospace Engineering Department at UCLA. He received his BS degree in Mechanical Engineering from the University of Wisconsin-Madison (1994), his MS and PhD degrees in Mechanical Engineering from Purdue University (1999, 2002). His research focuses on robot locomotion and manipulation, autonomous vehicles and humanoid robots. Hong's awards include the National Science Foundation's CAREER award, the SAE International's Ralph R. Teetor Educational Award, and the ASME Freudenstein/GM Young Investigator Award to name a few.

References

[1] Murphy R. Meta-analysis of autonomy at the DARPA robotics challenge trials. J. Field Rob. 2015;32:189–191.
[2] Lahr D. Design and control of a bipedal robot [dissertation]. Blacksburg (VA): Virginia Polytechnic Institute and State University; 2014.
[3] Park IW, Kim JY, Lee J, et al. Mechanical design of the humanoid robot platform. HUBO. Adv. Rob. 2007;21:1305–1322.
[4] Sakagami Y, Watanabe R, Aoyama C, et al. The intelligent ASIMO: system overview and integration. Proceedings of the IEEE Conference Intelligent Robots and Systems; 2002 Sep 30; Lausanne, Switzerland.
[5] Ogura Y, Lim H, Takanishi A. Development of a new humanoid robot WABIAN-2. Proceedings of the IEEE International Conference Robotics and Automation; 2006 May 15–19; Orlando, Florida.
[6] Lim H, Takanishi A. Biped walking robots created at Waseda University: WL and WABIAN family. Philos. Trans. A: Math. Phys. Eng. Sci. 2007;365:49–64.
[7] Gienger M, Loeffler K, Pfeiffer F. Towards the design of a biped jogging robot. Proceedings of the IEEE International Conference Robotics and Automation; 2001 May 15–19; Seoul, Korea.
[8] Gienger M, Loeffler K, Pfeiffer F. A Biped that Jogs. Proceedings of the IEEE International Conference Robotics and Automation; 2000 April 24-28; San Francisco, CA.
[9] Lohmeier S, Bushcmann T, Ulbrich H. Humanoid robot LOLA. Proceedings of the IEEE International Conference Robotics and Automation; 2009 May 11–17; Kobe, Japan.

[10] Taghirad HD. Robust torque control of harmonic drive systems. Montreal (QC), Canada: McGill University; 1997.
[11] Pratt J, Krupp B. Series elastic actuators for legged robots. Proceedings of the SPIE Unmanned Ground Vehicle Technology. 2004 Apr 12; Orlando, FL.
[12] Hobbelen DGE, Wisse M. Limit cycle walking. In: Humanoid robots and human like machines. Vienna; I-Tech Education and Publishing; 2007. Chapter 14, Limit Cycle Walking; p. 277–294.
[13] Pratt J. Exploiting inherent robustness and natural dynamics in the control of bipedal walking robots [dissertation]. Cambridge (MA): MIT; 2000.
[14] Chaitow L, Walker DeLany J. Clinical application of neuromuscular techniques: the lower body Vol 2. Edinburgh: Elsevier Health Sciences; 2002.
[15] Oshima T, Toroiumi K, Fujikawa T, et al. Effects of the lower leg bi-articular muscle in jumping. J. Rob. Mech. 2004;16:643–648.
[16] Lida F, Rummel J, Seyfarth A. Bipedal walking and running with spring-like biarticular muscles. J. Biomech. 2008;41:656–667.
[17] Salvucci V, Kimura Y, Oh S, et al. BiWi: bi-articularly actuated and wire driven robot arm. Proceedings of the IEEE International Conference Mechatronics; 2011 Apr 13–15; Istanbul, Turkey.
[18] Schenau GJVI. From rotation to translation: constraints on multi-joint movementsand the unique action of bi-articular muscles. Human Movement Sci. 1989;8: 301–337.
[19] Monsarrat B, Gosselin C. Workspace analysis and optimal design of a 3-leg 6-dof parallel platform mechanism. IEEE Trans. Rob. Autom. 2003;19:954–966.
[20] Voronov AV. The roles of monoarticular and biarticular muscles of the lower limbs in terrestrial locomotion. Human Physiol. 2004;30:476–484.